Received: May 24, 2024. Revised: June 20, 2024.

International Journal of
Intelligent Engineering & Systems

http://www.inass.org/

Dual-podal of Vivaldi Vehicular Antenna for IoV in 5G Communications

Bashar Mudhafar Ahmed[1,2]* **Laith Ali Abdul-Rahaim[2]**

[1]*Department of Electrical Engineering, College of Engineering, University of Babylon, Hilla, Babil, Iraq*
[2]*Department of Electronic and Communications Engineering,*
College of Engineering Al-Nahrain University, Jadriya, Baghdad, Iraq
* Corresponding author's Email: bashar.mudhafar.1@nahrainuniv.edu.iq

Abstract: Dual-podal of antipodal Vivaldi antenna has been designed, simulated, fabricated and measured. The antenna proposes a new design approach for dual-band to cover n78 and n96 frequency bands simultaneously which are used in a vehicle-to-anything (V2X). The n78 and n96 bands are used to provide a high speed with low latency connectivity in V2X communications, that ranging 3.3 GHz - 3.8 GHz and 6 GHz - 7 GHz, respectively. Dual-bands, high front to back ratio radiation, good directivity, and low-profile design are achieved. A vehicular proposed antenna simulated in free space and with the shark-fin radome then fabricated. The measurement frequencies 3.68 GHz and 6.44 GHz are achieved with a minimum reflection coefficient of -38.52 dB and -40.06 dB, respectively. Consequently, the maximum gain of 5.2 dBi and 6.9 dBi are obtained with 2.48 GHz and 0.98 GHz bandwidth, respectively. Simulation and measurement results is obtained with close agreements and comparison convergence. Moreover, the measurement results are compared with Modified Vivaldi antenna of quad-band based, Swastika-shaped gap-coupled patch of dual-band, and Dual-band SMMDG based MIMO. The proposed dual-podal antenna reveal to overcomes these works in terms of high matching impedance, bandwidth, and high front to back ratio with comparable size.

Keywords: Antipodal vivaldi antennas, Dual-podal antenna, Internet of vehicles (IoV), Vehicular antennas, Shark-fin.

1. Introduction

Due to the rapid and increasing demand for various wireless applications, the frequencies of V2X communications are required [1]. V2X allows to communicate between vehicles or a vehcile and the infrastructures around it. This V2X gives the vechile early knowledge of traffic signals [2], road congestion, road signs, status of other vehicles, and pedestrians. Therefore, V2X has the potential issue to make roads more safe and efficient [3].

Modern communication technologies have become significant interesting in data rates which allow high peaks with low latency among other advantages. Therefore, a dual and multi-band of compact planar antennas are the appropriate solution for the development of technologies in the V2X [3, 4]. Researchers use 3.5-GHz (3.3-3.8 GHz) for V2X applications [4-6]. Other researchers focus on 5G sub-band spectrum (6 - 7 GHz for America, Europe, and Japan while 5 - 6 GHz for the rest of global world) [7-9].

In recent decades, the 5G bands which includes the previous generations are developed [10, 11]. The new radio frequency (5G NR) V2X technology overcomes 5G sub-band spectrum and 3.5 GHz spectrum [12]. Therefore, the focus on these two bands is reqired to cover Internet of Vehcile (IoV) bands taking place towards the 6G [13, 14].

In this work, the V2X technology of 5G NR is used in order to cover IoV bands. Therefore, both bands, which are n78 (3.5 GHz) and n96 (5G sub-band), are distinctly covered. Accordingly, a dual-podal of Antipodal Vivaldi Antenna (AVA) shape is designed, simulated, and implemented. The simulation uses Computer Simulation Technology - Microwave Studio (CST-MW). The proposed antena contains two microstrip patch antenna layers to serve dual bands at the same feeding point with an air gab of 1.2 mm between them. In addition, three parallel-shaped line is inserted at the flare aperture at the GND

layer in the focal antenna's area as coplanar waveguide. The dual-podal dimensions are calculated using the conventional AVA antenna equations. Then, an optimization technique is employed to obtain resonant frequencies of 3.7 GHz and 6.5 GHz with matching impedance of -44.59 dB and -22.77 dB, respectively. Moreover, Front-to-Back (F/B) ratios of 3.08 and 16.94, and gains of 3.27 dBi and 7.82 dBi for each band are acheived. The antenna is optimized according to the fixed location at the shark-fin on the vehicle's roof. After fabrication process, the measurement and simulation results are compared and the comparison indicated good matching results between them. Furthermore, the proposed antenna is compared with three recently published works [6, 17, 18] in terms of operating frequency, bandwidth, matching impedance, gain, F/B ratio and other parameters. All these works are compatible with the IoV in NR 5G as well as 6G racing technological development.

The paper is organized as follows: Section 2 presents the proposed vehicular antenna design. Section 3 and 4 deal with the simulation and measurment results, respectivly, of the dual-podal Vivaldi antenna. Section 5 describes and summarizes the comparison between the measurement and simulation results. Finally, the results are discussed and concluded in section 6.

2. Antenna design

A dual wide band, low profile, high front-to-back ratio, good gain, scan angle capabilities, directivity over frequency, and suitable for shark-fin are required for IoV applications. Therefore, the antenna is designed to resonate at 3.7 GHz and 6.5 GHz to meet the requirements of IoV in New Radio (NR) 5G and beyond. Theoretical equations of AVA are used to estimate the center frequencies, substrate dimensions, the opening tapered curve, and other basic parameters. According to the variables limitation used in AVA theoretical equations, the results may not be accurate and dependable when used for the fabrication process. CST-MW is used to simulate, analyze, and optimize the proposed antenna design. This software is used due to the high number of variables required during simulation. In other words, the simulation results are more accurate and dependable in fabrication process.

In this paper, a new design technique is proposed with dual band coplanar waveguide (CPW) of AVA shape using the antipodal feed approach. It maintains a wide antenna bandwidth which covers the required bands of new 5G sub band services for vehicular roof top shark-fin applications. The antenna design provides two frequency bands with wide bandwidth of the resonant frequency to cover 3.3 GHz - 4.5 GHz and 6 GHz - 7 GHz of 5G sub band services simultaneously.

The proposed antenna design is based on dual layers. Each layer contains of flame retardant (FR-4) with 4.4 relative permittivity of dielectric constant (ε_r) and 0.025 of dielectric loss tangent (tan δ) coated by annealed copper of 0.035 mm on both sides, with dimensions 76 × 46 × 0.78 mm^3 (L x W x H). Dual bands are achieved by connecting these two AVA with the same 50 Ω feeding point using a Sub-Miniature version A (SMA) connector. The design is started by using the traditional equations of AVA in order to estimate the basic parameters of the desired antenna. The dimensions of the proposed antenna of this work are shown in Fig. 1. From Fig. 1, it can be shown that the two arms A and B represent the GND and patch layer, respectively. In the first layer, the distance between the dual-podal arms equals to 42.99 mm which is approximately equal to half of the wavelength of the 3.7 GHz. While in the second layer, the distance between the dual-podal arms equals to 45.45 mm which is approximately equal to the wavelength of the 6.5 GHz.

Fig. 2 shows both the front and back views of the antenna. It can be seen in Fig. 2 that there is a difference in the curvature of deviation according to the mathematical equations in order to get the two center frequencies of 3.7 GHz and 6.5 GHz. In order to increase the F/B ratio, a rectangle-shape was placed as a reflector located near the SMA connector with the same width of the FR-4 substrate. This reflector reduces the back and side lobes of the EM field propagation pattern. Consequently, the surface current is redistributed to increase the radiated power and reduce the sustained power on the patch surface. Moreover, the gain is raised by adding three parallel-shaped line as parasitic element that reduces the degradation of high frequencies without sacrificing the bandwidth.

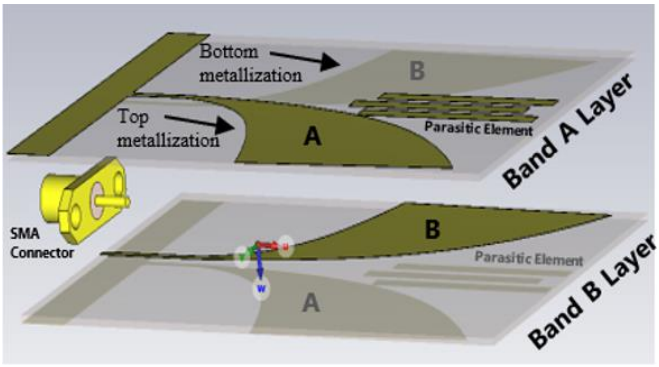

Figure. 1 Proposed antenna design of dual-band layers, where A is the GND layer and B is the patch layer

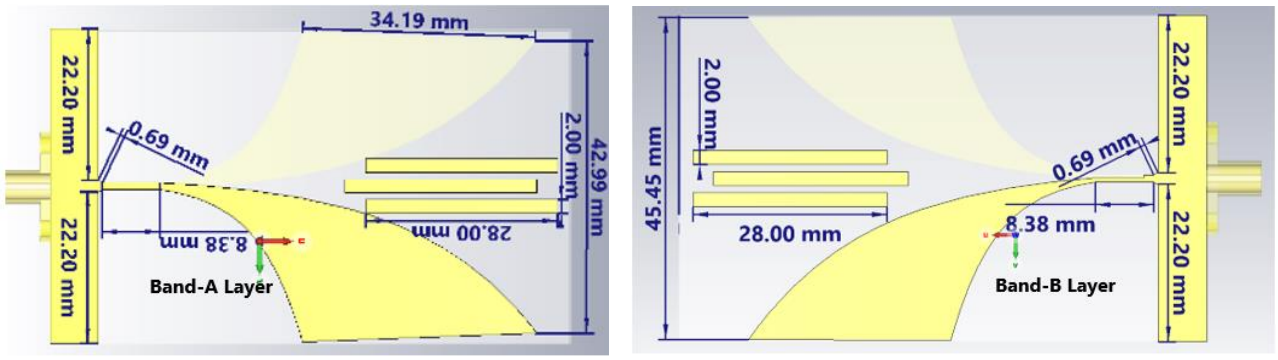

(a) (b)

Figure. 2 Proposed antenna design (dimensions in mm) of (a) band A and (b) band B

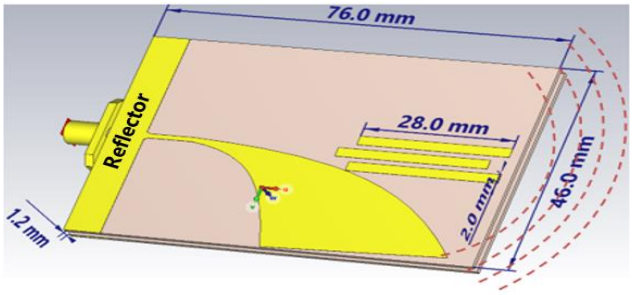

Figure. 3 Dual-podal radiation direction with reflector position

A three parallel-shaped line is inserted at the flare aperture between the two arms of planer layer (A and B). These lines allow a field coupling between the arms and produce a strong radiation at the end-fire direction. The design of the first layer of the antenna is applied to the second layer of it as well.

The proposed antenna, with its dimensions, is designed to work at a dual-band of frequencies which are n78 band (ranging from 3.3 GHz to 3.8 GHz) and n96 band (ranging from 6 GHz to 7 GHz) that are used for 5G bands. The geometry design of the antenna shown in Fig. 3 is comprised of dual-podal of two AVA antenna layers with 1.2 mm separation between them. Each outer face contains three parasitic elements (parallel-shaped line) with 28 mm x 2 mm dimensions as (L × W). The antenna dimensions 76 × 46 x 2.8 mm^3 (L x W x H) are designed with compact size to fit inside the shark-fin of the vehicle that mounted at the bottom end of the vehicle's roof. A vehicle voxel model is employed in CST-MW software to optimize the primary parameters values that are calculated from the conventional AVA equations. Other parameters can be extracted from CST-MW due to the use of finite element technique.

The traditional equations of AVA are shown below [6, 19]:

Tapered curve:

$$y_{out} = S_1 e^{R1} + A_1 \quad (1)$$

$$y_{in} = S_2 e^{R2} + B_1 \quad (2)$$

Length of the opening tapered curve:

$$S_1 = \frac{y_2 - y_1}{e^{R2} - e^{R1}} \quad (3)$$

$$S_2 = \frac{y_1 e^{R2} - y_2 e^{R1}}{e^{R2} - e^{R1}} \quad (4)$$

The length (L) of the AVA:

$$0.2\lambda \leq L \leq 0.5\lambda \quad (5)$$

Opening width of tapered curve:

$$2w < \frac{c}{fH\sqrt{\varepsilon_e}} - d \quad (6)$$

$$0.06\lambda \leq d \leq 0.09\lambda \quad (7)$$

Height of the substrate (H):

$$H \gg 0.003\lambda \quad (8)$$

Effective thickness of the conducting surface (t_{eff}):

$$0.005\lambda \leq (\sqrt{\varepsilon_e} - 1)t_{eff} \leq 0.03\lambda \quad (9)$$

The effective of dielectric constant (ε_e):

$$\frac{1}{2}(\varepsilon_r + 1) \leq \varepsilon_e \leq \varepsilon_r \quad (10)$$

Where λ, ε_r, (x_1,y_1), and (x_2 ,y_2) are represented the wavelength resonant frequency, dielectric constant, the starting and ending point of the exponential profile, respectively.

In order to resonate at the desired frequencies, an AVA is printed on two substrate layers with 0.78 mm thickness of FR-4 for each layer. These layers have the same dimensions exactly. However, each substrate has different AVA design. Moreover, the two patch layers are connected with a single SMA connector in which these two patches layer are connected as face to face with the SMA connector. While, the GND layers are the outer layers as shown in Fig. 3. In addition, the three parasitic element's structure is located in the focal antenna area of the GND layers to increase the CPW characteristic of the AVA. The exponentially tapered profiles offer an impedance change in order to reduce the transmitted power loss. For each layer, the width of the tapered end defines the lowest cutoff frequencies at the wavelength direction with parasitic element to increase antenna performance. Through the parameters study, the antenna bandwidth, radiation pattern, gain, matching impedance, and F/B ratio are evaluated.

3. Simulation results

By using the CST-MW software, the proposed antenna is placed on the outer end of the vehicle roof to ensure the clearest contact point with the consistent shape of a shark-fin. As shown in Fig. 4, the proposed antenna is at a distance of 5 mm from the car body to reduce contact with its metal surface. The simulation process followed by optimization technique to achieve good simulated results which are listed in Table 1.

In Table 1, it can be seen that the proposed antenna is designed to cover the n78 and n96 band that serve the 5G NR frequency bands applications. The proposed location of the dual-podal antenna is shown in Fig. 4. The designed antenna is resonated at the 5G NR frequency bands with high S_{11} value of the dual bands as shown in Fig. 5. The simulated results of F/B ratio and gain are shown in Fig. 6. The simulation reveals that the proposed antenna has good F/B ratio of 3.08 and 16.94 and maximum gain

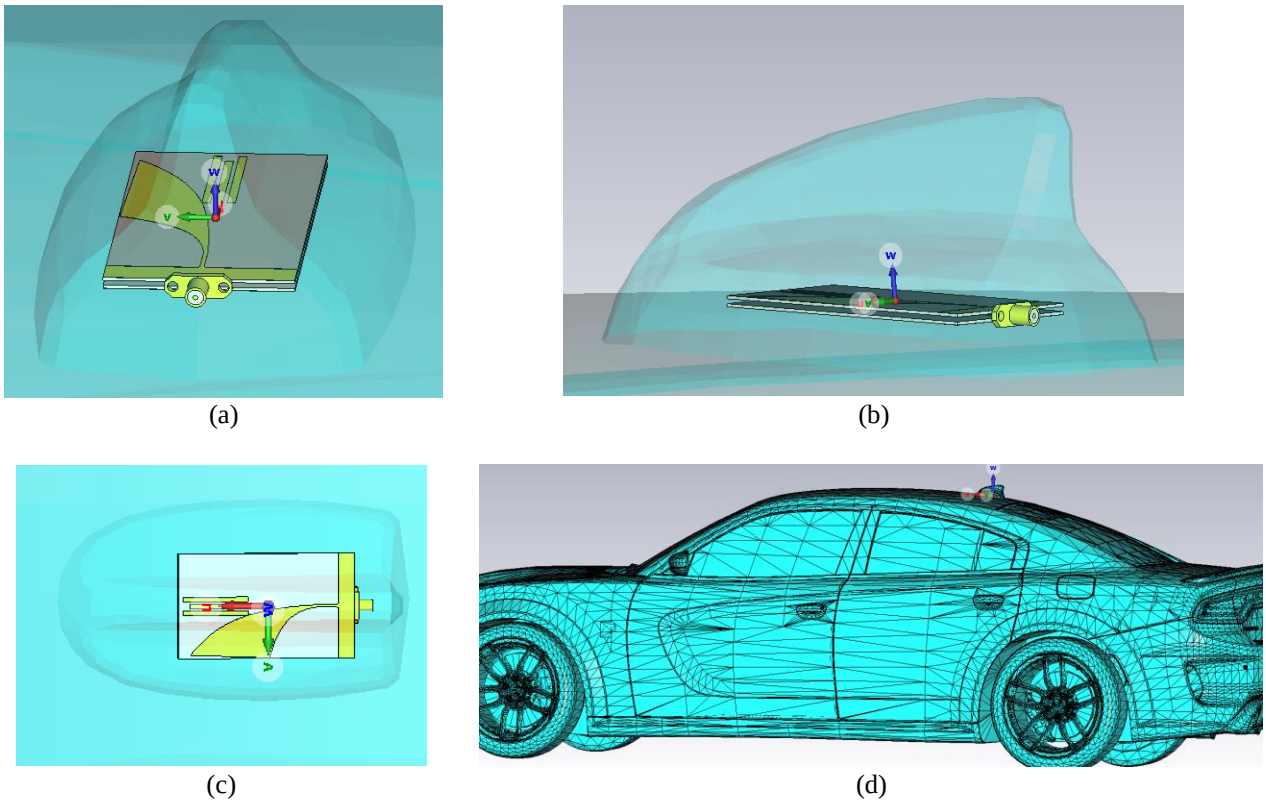

(a) (b) (c) (d)

Figure. 4 Proposed antenna location: (a) rear view, (b) side view, (c) top view, and (d) arrow shows the shark-fin radome position

Table 1. Simulated results of the shark-fin antenna.

Parameter (Unit)	Frequency band (GHz)	Bandwidth (GHz)	Matching impedance (dB)	Gain (dBi)	F/B	Linear Efficiency (%)	Dimensions (L × W × H) (mm^3)
Band A	3.3 - 4.5	1.2	−44.59	3.27	3.08	96.78	76×46×2.83
Band B	6 - 7	1	-22.77	7.82	16.94	98.98	76×46×2.83

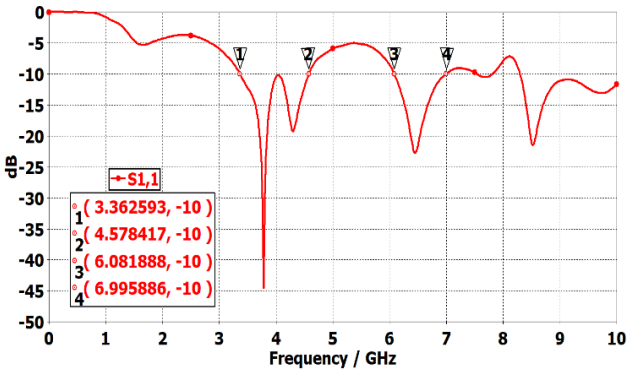

Figure. 5 Simulated return loss *S*11 of proposed antenna

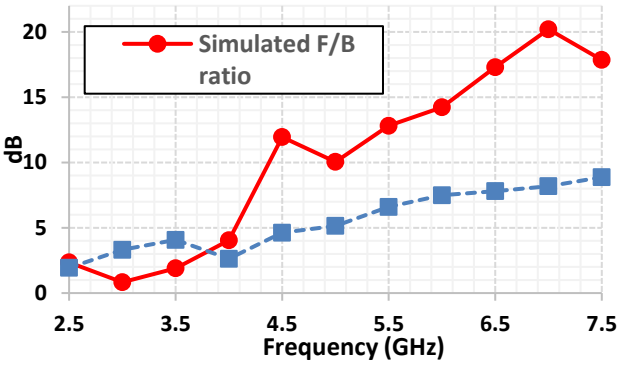

Figure. 6 Proposed antenna with simulated F/B ratio (solid line) and maximam gain (dashed line) over frequencies

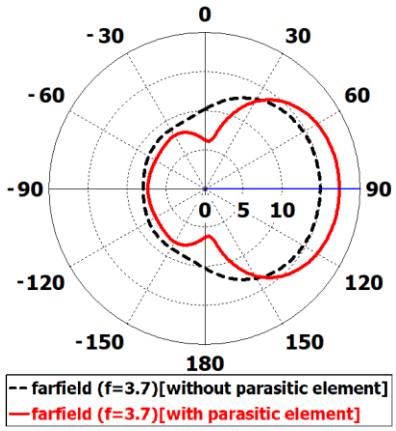

(a)

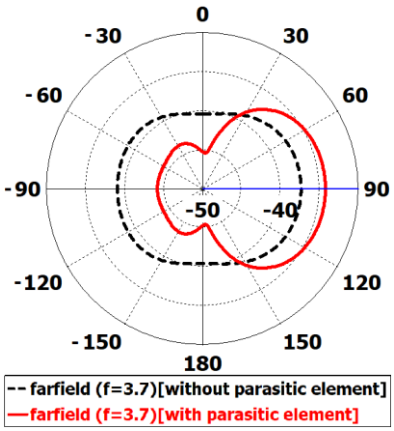

(b)

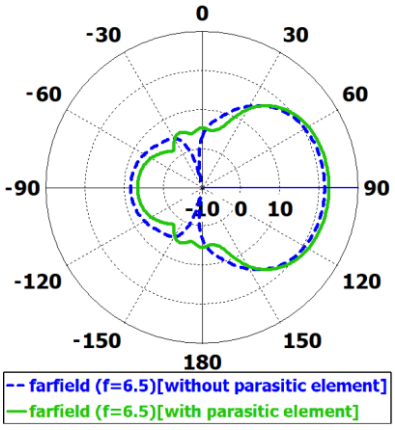

(c)

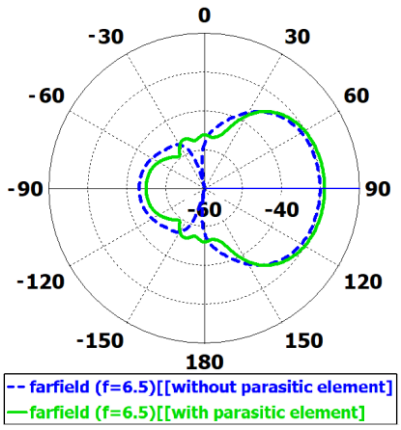

(d)

Figure. 7 The radiation patterns of farfield with (solid line) and without (dashed line) parasitic element at: (a) 3.7 GHz of E-plane, (b) 3.7 GHz of H-plane, (c) 6.5 GHz of E-plane, and (b) 6.5 GHz of H-plane

of 3.27 dBi and 7.82 dBi over the operating bands of 3.7 GHz and 6.5 GHz, respectively. The EM directivities of the two band are shown in Fig. 7. From Fig. 7, it can be shown that the main direction of the two band is achieved in 90°. In other words, the antenna works as an end - fire antenna with propagation at z-axis direction.

Finally, the simulation results indicated that the new antenna design proposed in this work has achieved the requirements of the desired application for transmitting or receiving the 5G frequency bands of n78 and n96.

4. Measurement setup

After achieving good simulation results, the photo-etched technique is used to fabricate the proposed antenna. The proposed dual-podal antenna is printed on substrate of FR-4, shown in Fig. 8, with thickness of 0.78 mm and permittivity of 4.4 + j 0.025. This type of substrate is considered as lossy material. However, many researchers are using this material due to its availability and low cost. It must be highlighted that the fabricated antenna has the same simulation dimensions.

The proposed design employed two layers of substrate; each substrate is used to work with one band of the desired frequency bands. From Fig. 9, it can be shown that there is a single SMA connector used to feed the dual-podal antenna as 50Ω port connection. The dual-podal antenna proposed in this work is fabricated and measured to evaluate the ability of the proposed antenna for achieving the requirements of the desired application.

As shown in Fig. 10, a measurement setup is used to measure all the practical parameters values, such as the resonant frequency, matching impedance, bandwidth, etc.; this setup contains Vector Network Analyzer (VNA), which is an Agilent model E5071C with two dual polarization horn antennas, frequency generator (Agilent model N5183A), frequency analyzer (Agilent model E4440A), and microwave absorber chamber.

The measurement has been done in the free space with using a real shark-fin as PVC enclosure. The measurement results are clarified and compared with the simulation results as well as with recently works in the next section.

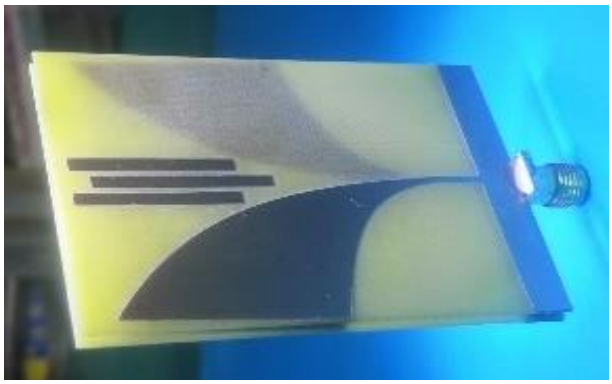

Figure. 8 Fabricated proposed dual-podal antenna

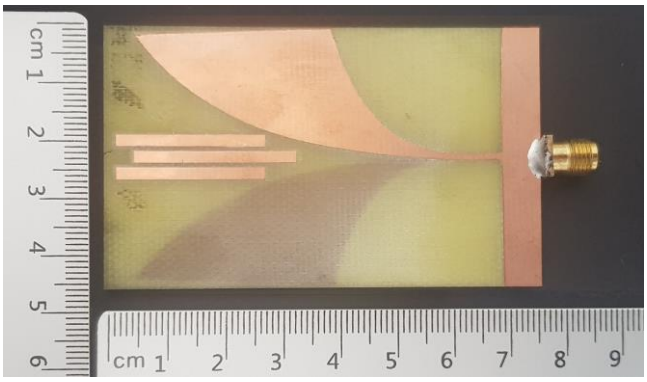

Figure. 9 Fabricated antenna dimensions

(a)

(b)

(c)

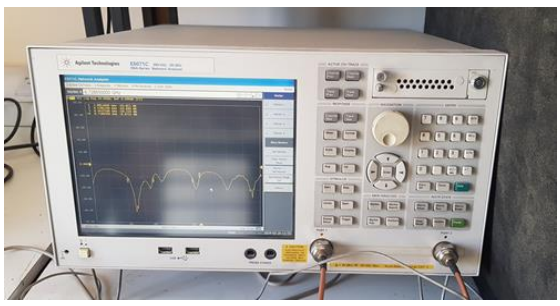

(d)

Figure. 10 Fabricated proposed antenna: (a) outside the shark-fin radome, (b) inside the shark-fin radome, (c) measurement setup, and (d) S_11measurement result

5. Comparison

Fig. 11 shows a comparison between the simulation and measurement results of S_{11} for the dual resonant frequency bands (Band-A and Band-B). From Fig. 11, it can be shown that the manufactured antenna covers the frequencies range of n78 and n96 band, with a slight difference between them.

From Table 2, it can be seen that the fabricated antenna has good matching results as compared to the simulation ones. The differences between these results are due to the limited number of variables which can be taken into the simulation process.

These good matching results are achieved due to the use of high mesh cells during the simulation process, real dimension of the substrate thickness, and the thickness of copper layer. Moreover, the value of relative permittivity which is used in CST-MW is measured by impedance analyzer. Furthermore, the SMA connector is simulated with the actual dimension rather than the use of auto generated port.

In order to evaluate the dual-podal antenna which is proposed in this work, a comparison is done between this work and recently published works. Table 3 summarizes the performance of the proposed antenna as compared to the measurement results of the compact multi-band antennas that serve NR 5G IoV band. Proposed antenna is compared with quad-band based modified Vivaldi antenna [6], dual-band swastika-shaped gap-coupled patch [17], and dual-band SMMDG based MIMO [18]. It should be noted that the antennas in [6, 17, 18] resonate more than one band. However, the proposed antenna covers LTE-4G and NR-5G frequencies and its suitability for the shark-fin radome of the vehicle.

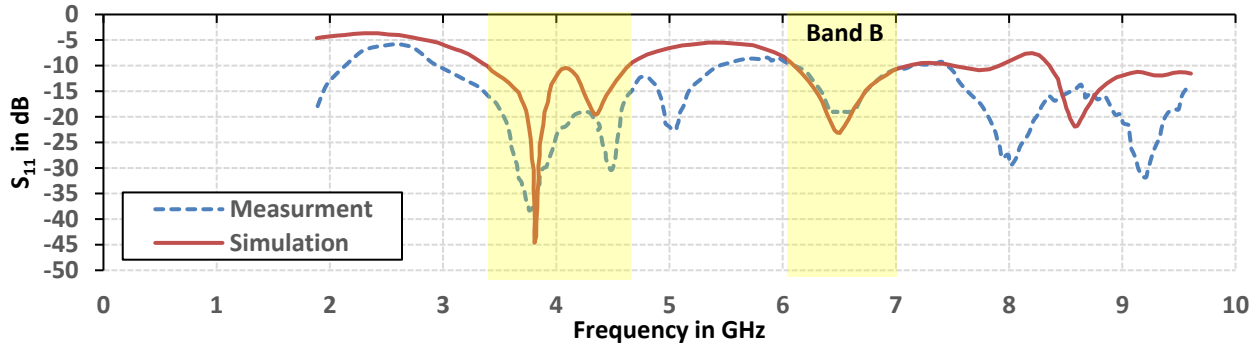

Figure. 11 Simulation and measurement comparison of S_{11} results

Table 2. A comparison between simulated and measurement results.

	Band	Resonant frequency (GHz)	S_{11} (dB)	Frequency band (GHz)	Bandwidth (GHz)	Gain (dB)
Simulation	A	3.78	-44.59	3.3 - 4.5	1.2	3.27
	B	6.5	-22.77	6 - 7	1	7.82
Measurement	A	3.7	-38.52	2.94 - 5.42	2.48	5.2
	B	6.44	-19.06	6.13 - 7.11	0.98	7.3

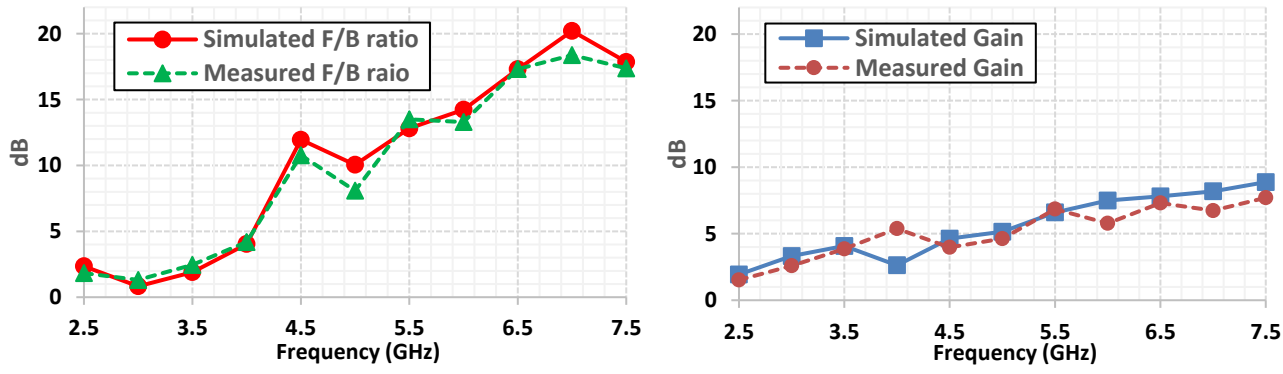

(a) (b)

Figure. 12 Proposed antenna with simulated (solid line) and measured (dashed line) of: (a) F/B ratio and (b) maximam gain over frequencies

Table 3. Comparison of the proposed antenna performance terms with similar frequency bands structures.

Reference	Operating Band	Frequency band (GHz)	Bandwidth (GHz)	Matching impedance (dB)	Gain (dBi)	F/B ratio	Sub strate	LTE-4G/NR-5G	Shark-fin compatible	Dimensions (L × W × H) (mm^3)
[6]	Quad band	3.64–4.08 4.15–5.40 5.58–6.16 6.51–7.32	0.41 1.21 0.59 0.41	-21 -28 -15 -13	7.5 6.4 8.5 7.2	- - - -	FR-4	Yes/Yes	Yes	118×85×1.5
[17]	Dual band	3.58-4.38 5.62-6.38	0.8 0.76	-26 -16	4.3 5.7	-	FR-4	No/Yes	Yes	16.9×16.9×1.57
[18]	Dual band	3.45-4.7 5.45-9	1.25 3.55	-13 -12	3.4 4	- - -	FR-4	Yes//Yes	Yes	31.5 ×45 ×1.6
This work	Dual band	2.94 - 5.42 6.13 - 7.11	2.48 0.98	-38.52 -19.06	5.2 7.3	3.12 17.31	FR-4	Yes/Yes	Yes	76×46×2.83

6. Discussion and conclusions

A two-layer of dual-band AVA patch antenna (dual-podal) is designed and studied experimentally to improve the bandwidth, matching impedance, gain, and directivity at n78 and n96 frequencies band region. By using a parasitic element design, the gain and directivity of the antenna are enhanced without compromising the bandwidth.

The proposed antenna is designed to operate at 3.7 GHz of n78 band and 6.5 GHz of n96 band for the NR 5G bands where IoV standard environment with a low profile, compatible size of shark-fin radome, and good matching impedance for dual bands.

The proposed antenna is fabricated using a rigid substrate of dual-podal AVA rather than flexible substrate. Especially, the mechanical support is required in this application. In addition, the resonant frequency and all antenna parameters will not be affected by the vibrations of the vehicle as compared to a flexible substrate.

From Table 3, it can be seen that the two main bands are focused on which are n78 and n96. The proposed antenna has a wider bandwidth than [6] by 0.87 GHz and 0.57 GHz and from [17] by 1.68 GHz and 0.22 GHz, respectively. Moreover, the bandwidth of the proposed antenna is wider than [18] by 1.23 GHz for the first band but less than it by 2.57 GHz for the other band. On the other hand, the proposed antenna is smaller in size than [6] by 5,151 mm^3 but larger than [17, 18] by 9,445 mm^3 and 7,625 mm^3, respectively.

The gain is one of the important parameters which is considered an issue for the small antenna size. The proposed antenna gain is less than [6] by 2.3 dBi and 1.2 dBi for the two bands of [6], respectively, that are located within the first band of the proposed antenna, but it is higher than [6] by 0.1 dBi within the second band of the proposed antenna. Moreover, the proposed antenna superior to [17] by 0.9 dBi and 1.6 dBi for the dual-bands and [18] by 1.8 dBi and 3.3 dBi, respectively. These results are considered comparable for the small size of the proposed antenna since the antenna is fabricated with the lossy material, FR-4. It is used for both layers of proposed antenna which is considered very cheap and available material. However, it is very difficult to design a highly efficient antenna using this material and maintain both bands.

The main important point is that the proposed antenna reaches a high performance of F/B with 3.12 and 17.31 for n78 and n96 bands, respectively, with good directivity. By increasing this ratio, signal-to-noise ratio is enhanced. This will increase the antenna's ability to focus its reception or transmission in a specific direction without using a reflector layer. Thus, the propagation field is directed outside the vehicle body. Consequently, the effective range is increased for the propagation field communication.

Therefore, the proposed antenna shows important features that is more applicable in IoV applications as compared to the quad-band based modified Vivaldi antenna, dual-band swastika-shaped gap-coupled patch, and dual-band SMMDG based MIMO in terms of bandwidth, matching impedance, and high F/B ratio with small antenna size.

Conflicts of Interest

The authors declare no conflict of interest.

Author Contributions

The paper conceptualization, methodology, software, validation, formal analysis, investigation, resources, data curation, writing—original draft preparation, writing—review and editing, and visualization have been done by the first author. The supervision and project administration have been done by the second author.

References

[1] M. Garcia, A. Molina-Galan, M. Boban, J. Gozalvez, B. Coll-Perales, T. Şahin, et al. "A Tutorial on 5G NR V2X Communications", *IEEE Communication Survey Tutorials*, Vol. 23, No. 3, pp. 1972-2026, 2021.

[2] M. Rafdzi, S. Mohamad, A. Ruslan, N. A. Malek, M. Islam, and A. Hashim, "Study for Microstrip Patch Antenna for 5G Networks", In: *Proc. of IEEE Student Conference on Research and Development*, Batu Pahat, Malaysia, pp. 524-528. 2020.

[3] J. Ahn, Y. Kim, and R. Kim, "A Novel WLAN Vehicle-To-Anything (V2X) Channel Access Scheme for IEEE 802.11p-based Next-Generation Connected Car Networks", *Switzerland Applied Sciences*, Vol. 8, No. 11, pp. 2112, 2018.

[4] G. Sree, K. Babu, S. Das, and T. Islam, "Design and Optimization of a Deep Learning Algorithm Assisted Stub-loaded Dual Band Four-port MIMO Antenna for Sub-6 GHz 5G and X band satellite communication Applications", *International Journal of Electronics and Communications*, Vol. 175, pp. 155074, 2024.

[5] T. Raj, R. Mishra, P. Kumar, and A. Kapoor, "Advances in MIMO Antenna Design for 5G: A Comprehensive Review", *Sensors*, Vol. 23, No. 14, pp. 6329, 2023.

[6] A. Kapoor, P. Kumar, and R. Mishra, "High Gain Modified Vivaldi Vehicular Antenna for IoV Communications in 5G Network", *Heliyon*, Vol. 8, No. 5, p. e09336, 2022.

[7] Z. Qadir, K. Le, N. Saeed, and H. Munawar, "Towards 6G Internet of Things: Recent advances, use cases, and open challenges", *ICT Express of Korean Institute of Communications and Information Sciences*, Vol. 9, No. 3, pp. 296-312, 2023.

[8] Y. Xu, T. Bai, Z. Zhang, A. Wang, C. Cui, and J. Hou, "A Compact Multi-Band Monopole Antenna for 5G NR Coal Mine Applications", *Progress in Electromagnetics Research Letters*, Vol. 115, pp. 57-62, 2024.

[9] C. Yen, D. Sim, "Novel techniques applied to MIMO antenna array for 5G sub-7 GHz smartphone applications", In: *Proc. of IEEE of International Workshop on Antenna Technology*, Aalborg, Denmark pp. 1-2, 2023.

[10] K. Sehla, T. Nguyen, G. Pujolle, and P. Velloso, "Resource Allocation Modes in C-V2X: From LTE-V2X to 5G-V2X", *IEEE Internet of Things Journal*, Vol. 9, No. 11, pp. 8291-8314, 2022.

[11] GSMA WRC Series, *3.5 GHz in the 5G Era*, pp. 1-10, 2021.

[12] X. Wan, C. Sun, F. Jiang, J. Wang and J. Jiang, "Prediction of mmWave BS Layout by DNN with Sub-6GHz Band Features", In: *Proc. of IEEE International Conference on Consumer Electronics*, Las Vegas, NV, USA, 2023.

[13] S. Gyawali, S. Xu, Y. Qian, and R. Q. Hu, "Challenges and Solutions for Cellular Based V2X Communications", *IEEE Communications Surveys and Tutorials*, Vol. 23, No. 1, pp. 222-255, 2021.

[14] S. Ibrahim, M. Singh, S. Salem, H. Ibrahim, M. Islam, S. Islam, A. Alzamil, and W. Abdulkawi, "Design, Challenges and Developments for 5G Massive MIMO Antenna Systems at Sub 6-GHz Band: A Review", *Nanomaterials*, Vol. 13, No. 3, pp. 520-560, 2023.

[15] M. Dvorsky, H. Ganesh, and S. Prabhu, "Design and Validation of an Antipodal Vivaldi Antenna with Additional Slots", *Int J Antennas Propag*, Vol. 2019, pp. 1-10, 2019.

[16] A. Ruddle, "Influence of Dielectric Materials on In-Vehicle Electromagnetic Fields", In: *Proc. of IET Seminar on Electromagnetic Propagation in Structures and Buildings*. London, 2008.

[17] Z. Zhang, M. Li, Q. Dai, M.-C. Tang, and L. Zhu, "Compact, Wideband, Dual-Band Polarization and Pattern Diversity Antenna for Vehicle Communications", *IEEE Transactions on Antennas and Propagation*, Vol. 71, No. 5, pp. 4528-4533, 2023.

[18] W. A. Neamah, H. M. A. Sabbagh, and H. Al-Rizzo, "A Compact Two-Element Linearly and Orthogonal Circularly Polarized MIMO Antenna System for 5G Cellular and WLAN/Wi-Fi 6E Application", *IEEE Access*, Vol. 11, pp. 96879-96891, 2023.

[19] N. Sathishkumar, V. Nandalal, and R. Natarajan. "Design of Dual Mode AVA with Enhanced Radiation Characteristics", *Springer*, Vol. 125, pp. 3249-3259.